communications in mathematical
match
and in computer chemistry

no. 44, October 2001

MATCDY (44) 117 - 133 (2001)

ISSN 0340 - 6253

TORANES VERSUS TORENES

Mircea V. Diudea,[a*] Ioan Silaghi-Dumitrescu[a] and Bazil Parv[b]

[a] Faculty of Chemistry and Chemical Engineering
[b] Department of Computer Science, Faculty of Mathematics
Babes-Bolyai University, 3400 Cluj, Romania

Abstract Construction of polyhex and other tiled tori starting from square-like tori is presented. Leapfrog transformation of both linear and angular polyhex isomers is discussed and illustrated. Molecular mechanics and semi empirical calculations emphasize toranes (alkanes-like hydrocarbons) rather torenes (alkenes-like or arenes-like molecules) as plausible candidates to the real molecule status.

INTRODUCTION

Fullerene chemistry is nowadays a well-established field of both theoretical and experimental investigations. The initial fascinating appeal, coming from their beautiful symmetry [1-3] shifted later to real chemistry. [4-6] Carbon allotropes with finite molecular cage structures have been functionalized or inserted in supramolecular assemblies. [7-9]

Since a spherical surface cannot be tiled by pure hexagonal pattern, [10,11] the scientists looked for other surfaces capable to allow a full polyhex tessellation. Such surfaces are cylinders (e.g., open nanotubes) and tori, [12-20] both of them identified in the products of laser irradiation of graphite. [21,22] According to Euler's formula: $v - e + f = 2 - 2g$ (v, e, f, g being respectively the number of vertices, number of edges, number of faces, and genus) a torus is of genus one while a sphere or a cylinder are of genus zero. Formula is useful for

---

Dedicated to Professor A. T. Balaban on his 70th anniversary, for his bright contribution to Chemical Graph Theory.

checking the consistency of an assumed structure.

This paper describes a novel way of generating polyhex tori, starting from quadrilateral tessellated tori. Leapfrog transformation along with the energetic characterization of some classes of tori is presented.

CONSTRUCTION OF POLYHEX TORI

Covering a toroidal surface by hexagons is related to the tessellation of an equivalent planar parallelogram. [11, 16,18] The resulting polyhex lattice is completely defined by four independent integer parameters, reducible to three parameters: [19] a torus $\mathbf{T}_{p,q,t}$ is obtained from p x q hexagons stacked in a p x q-parallelogram, whose opposite edges are glued in order to form a tube. Next, the two ends of the tube are glued together, eventually rotated by t hexagons before gluing, to form the torus.

An alternative to the parallelogram procedure is the use of adjacency matrix eigenvectors in finding appropriate triplets, i.e., 3D coordinates of a graph (in particular, a torus). [23] The method was previously used in generating spheroidal fullerenes. [24,25]

Our construction starts from a quadrilateral net embedded on the toroidal surface, generated according to an elementary geometry (see our previous work [26]). A torus $\mathbf{T}_{c,n}$ is a lattice obtained by circulating a c-membered cycle along another cycle: its n images together with the edges joining (point by point) the subsequent images form a polyhedral torus tiled by some square patterns. The problem is to change the quadrilaterals into hexagons or other tiling patters, suitable from chemical point of view. In this respect, we developed several cutting procedures.

Standard C_6 cutting.

A cutting operation consists of deleting appropriate edges in a square-like net in order to produce some larger polygonal faces. By deleting each second *horizontal* edge and alternating edges and cuts in each second row it results in a standard h,C_6 *pattern* (Figure 1, a).

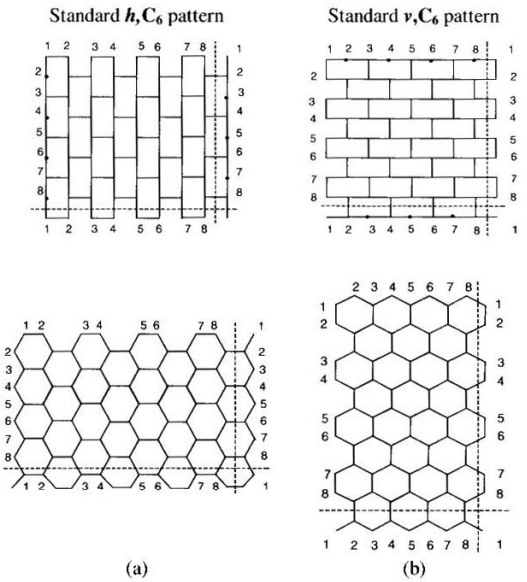

FIGURE 1. Standard $\mathbf{C_6}$ patterns and their optimized forms.

After optimizing by a molecular mechanics program, phenanthrenoid, hexagonal pattern appears on the torus. Figure 2 illustrates an idealized polyhex torus. However, after optimization, the surface becomes flattened (see below).

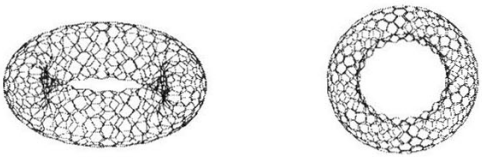

FIGURE 2. $\mathbf{T}_{20,40,C6}$ (idealized): (a) side view; (b) top view.

By following the same algorithm as above, but operating vertically, a standard v,C_6 pattern (Figure 1, b) is generated. It means that after optimization an anthracenoid isomeric pattern is obtained.

Note that each hexagon consumes exactly two squares in the square-like net. By construction, the number of hexagons in the h,C_6 *pattern* is half the number of squares on dimension c of the torus $T_{c,n}$ while in the v,C_6 *pattern* the reduced number of hexagons appears on dimension n. Recall that, the above cutting procedure *leaves unchanged the number of vertices in the original square-like torus.*

The name of a polyhex torus, thus generated, has to remind the *type of cutting*, h or v, as well as the *cycle membering*.

OTHER PATTERN CONSTRUCTIONS

In tessellating a toroidal surface, some other patterns have been considered. An alternating C_4,C_8 pattern was depicted in ref. [13] (see also ref. [27]). In our procedure, this pattern results by following the principle of alternating edges and cuts and keeping the same any two subsequent rows. The cutting illustrated in Figure 3 is performed horizontally. This pattern was previously used for tiling spherical fullerenes. [28]

In order to reduce the strain tension in pure polyhex tori, a number of pentagons and heptagons were introduced. [23] When a pure C_5,C_7 pattern is used, the lattice is called

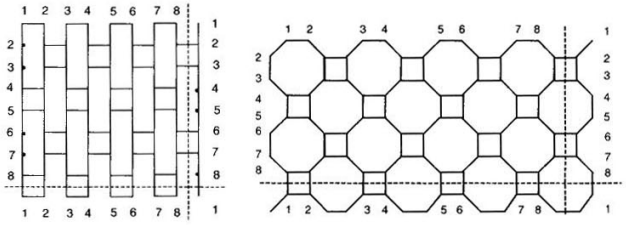

FIGURE 3. A C_4,C_8 pattern and its optimized form.

azulenoid. [13] The pentalene (i.e., two fused five-membered rings) apparition is not a backtracking in tori, since a more pronounced curvature occurs in such structures (see below), in comparison with the spheroidal fullerenes.

In our procedure, the construction of a pure $\mathbf{C_5,C_7}$-pattern needs four vertex rows (i.e., a (0 mod 4) lattice – Figure 4). In case of a (2 mod 4) network it results in a $\mathbf{C_5,C_6,C_7}$-pattern (Figure 5).

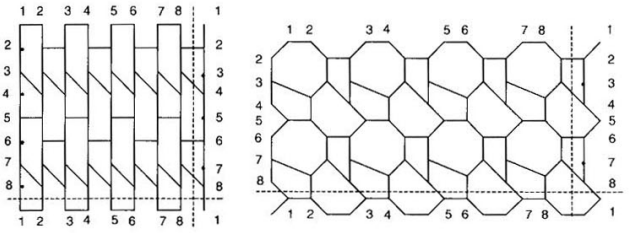

FIGURE 4. A $\mathbf{C_5,C_7}$-pattern

In the above constructions, non-twisted square lattices are used. We stress here that, excepting the patterns involving C_5 and C_7, our tori are non-twisted lattices (see below). This fact is in contrast to the parallelogram procedure, where, even for $t = 0$ (see above), some twisting (e.g., by an angle of pi / 6) appears.

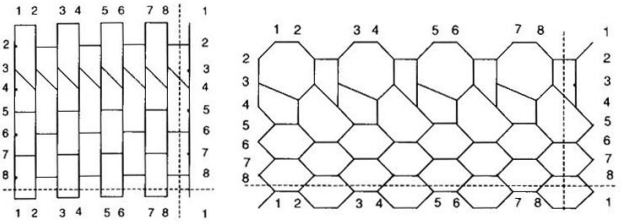

FIGURE 5. A $\mathbf{C_5,C_6,C_7}$-pattern

Let now consider a twisted square-like lattice (Figure 6) and follow the above principle of cutting. Different patterns appear, function of the number of vertex rows affected by twisting. In case of an odd number of twisted rows (denoted here by t_1), two rows of alternating C_4, C_8 polygons appear among the C_6 ones. Conversely, when the number of rows is even (marked by t_2), pure $\mathbf{C_6}$ pattern results.

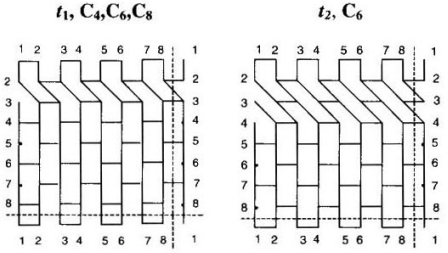

FIGURE 6. Patterns resulted by cutting procedure in odd and even number of vertex rows , respectively.

The optimized form of these patters will be illustrated below.

LEAPFROG TRANSFORMATION OF POLYHEX TORI

The *leapfrog* transformation of a map (i.e., a combinatorial representation of a closed surface) involves the omnicapping (i.e. stellation) of its faces followed by dualization. [29-32]

Omnicapping a map consists of adding a new vertex in the center of each face and connecting it with each vertex of the face boundary. *Dualization* is accomplished by locating a point in each face and joining two points if their corresponding faces have a common edge. Within leapfrogging, the dualization is made on the stellated transform of the map.

In polyhex tori, two cases appear, function of the starting lattice: $\boldsymbol{h}$,$\mathbf{C_6}$ and $\boldsymbol{v}$,$\mathbf{C_6}$. The dualization step will decide the type of the leapfrog product.

(a) Case of $\boldsymbol{h}$,$\mathbf{C_6}$-*pattern* (i.e., phenanthrenoid-): the product is an anthracenoid net. In our approach, it is equivalent to a $\boldsymbol{v}$,$\mathbf{C_6}$-pattern. The leapfrog process acts in the sense of expanding (three times) the $\boldsymbol{n}$-dimension of a torus. Figure 7 illustrates the stages occurring in

the leapfrog transformation of an h,C_6 net. It appears more clear after geometry optimization, as illustrated in Figure 8: a pure, non-twisted, v,C_6-patterned, $T_{8,24,v,C6}$ is obtained from the smaller, h,C_6-patterned, $T_{8,\ 8,h,C6}$.

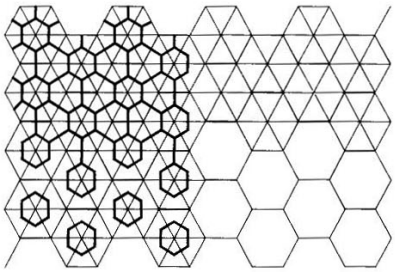

FIGURE 7. Stages in the leapfrog transformation of a h,C_6 -pattern

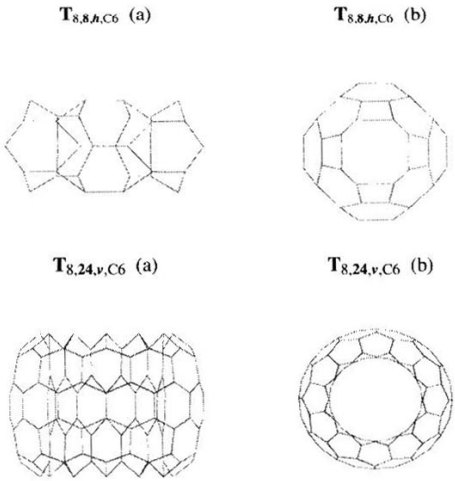

FIGURE 8. Leapfrog transformation of type 3*n: $T_{8,\ 8,h,\ C6} \rightarrow T_{8,\ 24,v,\ C6}$

(b) Case of ν,C_6-*pattern* (i.e., anthracenoid-): the product is now a phenanthrenoid, h,C_6-patterned, net (Figure 9). In this case, the leapfrog transformation acts by expanding (three times) the c-dimension of a torus (see above).

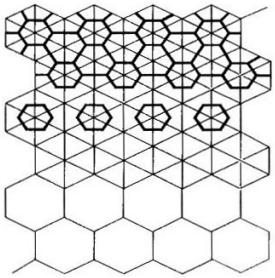

FIGURE 9. Stages in the leapfrog transformation of a ν,C_6 -pattern

Figure 10 gives a nice example in this respect. Observe that, as the c-dimension increases, the torus becomes more flattened, in contrast to the "idealized" polyhex torus, given in Figure 2.

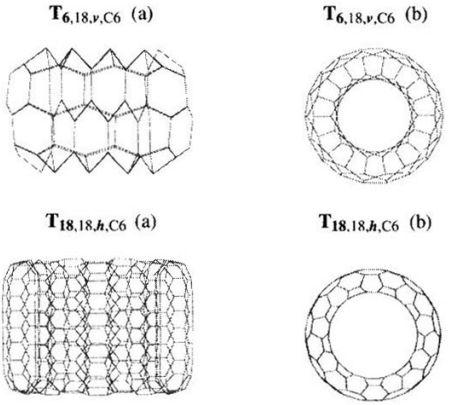

Figure 10. Leapfrog transformation of type 3*c: $T_{6,18,\nu,C6} \rightarrow T_{18,18,h,C6}$

Concluding, the leapfrog transformation of the non-isotropic polyhex net leads to the mutual interchanging of its twin patterns: h,C_6 and v,C_6, respectively. Different stability is expected for the different phenanthrenoid and anthracenoid isomers (as shown in the next sections).

MOLECULAR MECHANICS COMPUTATIONS

As a consequence of diverse pattern covering a toroidal surface, several isomers (i.e., different patterned lattices) are expected for a given $T_{c,n}$ torus. Our computer program enabled us to generate tori up to 1000 vertices, with the above described tessellation. The interest is now to find structures plausible from the point of view of chemistry, i.e., *plausible molecules*.

In a first approximation, we calculated the total energy, as provided by molecular mechanics calculations. The structures considered here (and illustrated below) are isomers of $T_{8,24}$, having 8 x 24 = 192 vertices (e.g., carbon atoms). They are sufficiently large to minimize the strain energy given by a more pronounced curvature of a toroidal, compared to a spherical surface. Each structure is given as side view (a) and top view (b).

$T_{8,24,h,C6}$ (a)

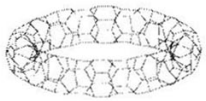

$T_{8,24,h,C6}$ (b)

$T_{8,24,h,C4,C8}$ (a)

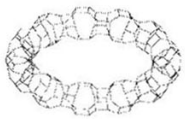

$T_{8,24,h,C4,C8}$ (b)

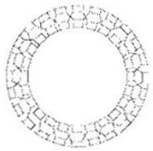

The value exhibited by $\mathbf{T}_{8,24,h,C4,C8}$ (entry 6) is a normal one, since small, strained C_4 rings are present.

The mixed pattern C_5,C_6,C_7 was considered as an *abnormality* statistically favored to occur in a polyhex isomer, particularly in large structures. This pattern, as well as the full C_5,C_7 lattice show a some degree of twisting, in comparison to the standard C_6 patterns. However, in case of C_5,C_6,and C_7 pattern the strain energy (Table 1, entry 8) is even lower than that exhibited by the polyhex isomers (Table 1, entries 2 and 4). Among the non-twisted structures, $\mathbf{T}_{8,24,\nu,C6}$ (entry 4) shows the highest energy (equivalent with highest instability).

The twisted structures, of t_1,h,C_4,C_6,C_8 and t_2,h,C_6 type (Table 1, entries 12 and 14) exhibit a normal higher level of energy.

Interesting results we obtained when considered perhydro-tori, i.e., *toranes*, named by analogy to alkanes, or totally hydrogenated hydrocarbons. Such structures, with no *pi* bonds, show low reactivity (paraffinum, in Latin) and any aromatic character (see the next section).

$\mathbf{T}_{8,24,h,C5,C6,C7}$ (a)

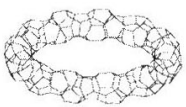

$\mathbf{T}_{8,24,h,C5,C6,C7}$ (b)

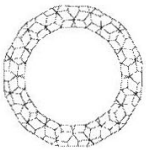

$\mathbf{T}_{8,24,h,C5,C7}$ (a)

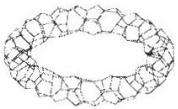

$\mathbf{T}_{8,24,h,C5,C7}$ (b)

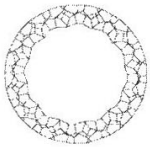

Normal toranes, e.g., those in entries 1, 7, 9, 11 and 13 of Table 1 exhibit a lower energy (i.e., a higher stability), in comparison with the corresponding pure carbon tori. In case

of $T_{8,24,v,C6}$ the hydrogenation results in an exacerbating instability, suggesting a more eclipsed disposition of the hydrogen atoms.

An evaluation of lattice dimensions is possible, from the optimized geometries. Data, given in Table 1 are: internal diameter d_{int}, external diameter d_{ext}, wall thickness w and height h (in Angstroms). In case of hydrogenated structures, the lattice dimensions refer to the skeleton only, the hydrogen atoms being disregarded. Even so, the lattice appear as somewhat expanded, and no exception was observed.

$T_{8,24,t1,h,C4,C6,C8}$ (a)

$T_{8,24,t1,h,C4,C6,C8}$ (b)

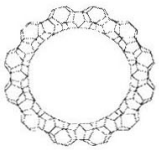

$T_{8,24,t2,h,C6}$ (a)

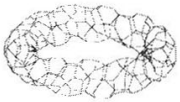

$T_{8,24,t2,h,C6}$ (b)

TABLE 1. Data for T8,24; Energy E (MM+; Kcal/mol), Internal Diameter d_{int}, External Diameter d_{ext}, Wall Thickness w and Height h (in Angstroms)

No	Torus	E	d_{int}	d_{ext}	w	h
1	8,24,h,C_6,H	2799.95	14.20	20.76	3.28	3.93
2	8,24,h,C_6	3544.04	12.94	18.67	2.87	3.54
3	8,24,v,C_6,H	9712.50	7.42	12.16	2.82	7.33
4	8,24,v,C_6	5097.72	7.14	11.70	2.37	7.90
5	8,24,h,C_4,C_8,H	4655.41	14.74	20.36	3.16	3.37
6	8,24,h,C_4,C_8	3749.46	14.25	19.70	3.12	3.52
7	8,24,h,C_5,C_6,C_7,H	2293.57	14.10	20.30	3.27	3.62
8	8,24,h,C_5,C_6,C_7	3081.14	13.61	19.26	3.06	3.40
9	8,24,h,C_5,C_7,H	4164.33	14.92	21.67	3.39	3.69

10	8,24,h,C_5,C_7	4529.23	13.82	19.82	2.67	3.13
11	8,24,t_1,h,C_4,C_6,C_8H	4050.41	14.77	21.02	3.34	3.71
12	8,24, t_1,h,C_4,C_6,C_8	4491.98	12.76	19.12	3.43	3.15
13	8,24,t_2,h,C_6H	5694.79	11.44	18.97	3.87	3.80
14	8,24, t_2,h,C_6	7381.00	9.92	17.01	3.89	3.79

At the end of this section, two polyhex tori, showing complementary dimensions, as a possible assembly of isomers, is presented in Figure 11. The dimensions are as follows:

$\mathbf{T}_{20,30,C6}$ (d_{int} = 18.18; d_{ext} = 23.56; w = 2.69; h =10.73)

$\mathbf{T}_{30,20,C6}$ (d_{int} = 11.42; d_{ext} = 16.61; w = 2.65; h =16.90)

Some enlarged d_{int} = 19.66 of $\mathbf{T}_{20,30,C6}$ is plausible to accept the guest ($\mathbf{T}_{30,20,C6}$ of d_{ext} = 16.61) into its hall to form a double layer (of 1200 atoms) assembly.

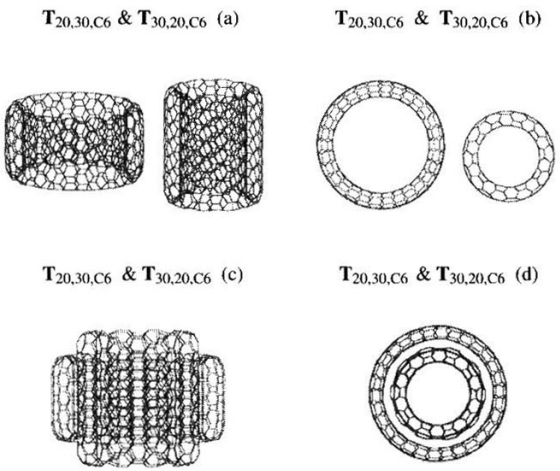

FIGURE 11. A double layer assembly of 1200 atoms

SEMIEMPIRICAL COMPUTATIONS

A *preferable* fullerene [29] obey, in others, the *isolated pentagon rule*. [33,34] It means that, for higher stability, a trivalent structure, embedded on a closed sphere-like surface, should avoid strained or antiaromatic rings, such as triangles, squares or abutting pentagons (i.e., pentalene), the boundary of which is a 8-membered, antiaromatic cycle. Four membered rings on the surface of fullerenes are, however, not completely excluded as recent molecular orbital calculations have shown [28,35] Actually, heterofullerenes containing only four and six membered rings could be even more stable than their carbon analogues [36-38].

In order to asses the effect of other than six membered rings on the surface of these tori as well as that of the saturation, we have performed semiempirical molecular orbital calculations at the PM3 level on a set of $T_{8,24}$ systems. Table 2 summarizes the results of single point calculations (at the geometry obtained at the mm+ level) on various members of this series along with those obtained after full optimization at the PM3 level.

Some remarks impose:

(a)Toranes are far more stable than the corresponding pure carbon structures (see Tables 1 and 2); this fact is in line with the results of ab initio and semiempirical calculations carried out on the fullerene-fullerane systems. [38,39]

The HOMO-LUMO gaps (both for the single point calculated as well as the optimized species) increase on going from torenes to toranes, suggesting a kinetic stabilization. This finding can be interpreted in terms of localization of the surface electron pairs of torenes in the C-H bonds of toranes with the subsequent diminution of the surface interelectronic repulsions.

(b) Data suggest that the C_5,C_6,C_7 systems (Table 2, entries 5, 6 and 14, 15) should be thermodynamically more stable than other isomers (of $\mathbf{T}_{8,24}$) containing pure (C_4,C_8), (C_6) or (C_5,C_7) lattices.

This result is in agreement with those obtained by other authors, [18,23] which showed that insertion of equal number of pentagonal and heptagonal defects might reduce the strain energy.

TABLE 2. PM3 Calculation for $\mathbf{T}_{8,24}$ of Various Patterns: Enthalpy of Formation ΔH_f (kcal/mol) HOMO, LUMO and HOMO-LUMO Gap HL-G (eV):

	Torus $\mathbf{T}_{8,24}$	ΔH_f	HOMO	LUMO	HL-G
1	$\boldsymbol{h}$,C_6,H	2554.00	-9.108	1.105	10.213
2	$\boldsymbol{h}$,C_6,H*	2403.50	-9.010	0.650	9.660
3	$\boldsymbol{h}$,C_4,C_8,H	2518.09	-9.707	1.126	10.833
4	$\boldsymbol{h}$,C_4,C_8,H*	2289.55	-9.500	1.240	10.740
5	$\boldsymbol{h}$,C_5,C_6,C_7,H	1974.57	-9.170	1.898	11.068
6	$\boldsymbol{h}$,C_5,C_6,C_7,H*	1811.93	-9.120	1.960	11.080
7	$\boldsymbol{h}$,C_5,C_7,H	4264.05	-9.175	0.766	9.940
8	$\boldsymbol{t}_1$,$\boldsymbol{h}$,C_4,C_6,C_8,H	7299.98	-8.658	1.727	10.585
9	$\boldsymbol{t}_2$,$\boldsymbol{h}$,C_6,H	14039.06	-7.079	0.662	7.741
10	$\boldsymbol{h}$,C_6	7114.86	-7.848	-4.235	3.613
11	$\boldsymbol{h}$,C_6 *	6301.44	-8.062	-3.790	4.272
12	$\boldsymbol{h}$,C_4,C_8	8913.97	-8.308	-4.629	3.679
13	$\boldsymbol{h}$,C_4,C_8 *	7036.41	-9.031	-2.492	6.539
14	$\boldsymbol{h}$,C_5,C_6,C_7	6906.63	-9.126	-4.276	4.850
15	$\boldsymbol{h}$,C_5,C_6,C_7 *	5790.62	-9.122	-2.951	6.171
16	$\boldsymbol{h}$,C_5,C_7	11293.72	-9.035	-3.998	5.037
17	$\boldsymbol{t}_1$,$\boldsymbol{h}$,C_4,C_6,C_8	9757.10	-8.494	-4.273	4.221

Values corresponding to the optimized structures at the PM3 level

The semiempirical PM3 [40] calculations have been carried out by using SPARTAN 5.0 package [41] on an Octane Silicon Graphics machine, and GAMESS-US [42] installed under LINUX on a Pentium III system.

Molecular mechanics (mm+ force field) optimizations have been performed by using HyperChem 4.5 from HyperCube. [43]

CONCLUSIONS

Toroidal fullerenes, along with tubulenes and classical spherical fullerenes became a subject of intensive research beyond the molecular frontiers. A third way in constructing tori, namely by transforming a square-like net (embedded onto a toroidal surface) into polyhex and/or variously tiled lattices, is added to the well-known graphite zone-folding and adjacency matrix eigenvector procedures. The structures thus generated become plausible candidates to the real molecule status as soon as they are optimized by a molecular mechanics or, better, by a quantum chemical computer program. Preliminary data enabled us to propose toranes (fully hydrogenated) rather than torenes (aromatic or olefinic) as possible chemical tessellating of a toroidal surface. Further research is directed towards finding the equivalence of our structures to the canonical representation [11] and construction of aggregate supramolecular assemblies.

REFERENCES

[1] Kroto, H. The first predictions in the Buckminsterfullerene crystal ball. *Fuller. Sci. Technol.* **1994**, *2*, 333-342.

[2] King, R. B. Unusual permutation groups in negative curvature carbon and boron nitride structures. *Croat.Chem. Acta*, **2000**, *73*, 993-1015.

[3] Hosoya, H.; Tsukano, Y. Efficient way for factorizing the characteristic polynomial of highly symmetrical graphs such as the Buckminsterfullerene. *Fuller. Sci. Technol.* **1994**, *2*, 381-393.

[4] Zorc, H.; Tolić, Lj. P.; Martinović, S.; Srzić, D. Synthesis and laser desorption Fourier transform mass spectrometry of massive fullerenes. *Fuller. Sci. Technol.* **1994**, *2*, 471-480.

[5] Diedrich, F. Thilgen, C. Covalent Fullerene Chemistry, *Science*, **1996**, *271*, 317-323.

[6] Neretin, I. S.; Lyssenko, K. A.; Antipin, M. Yu.; Slovokhotov, Yu. L.; Boltalina, O. V.; Troshin, P. A.; Lukonin, A. Yu.; Sidorov, L. N.; Taylor, R. $C_{60}F_{18}$, a flattened fullerene: alias a hexa-substituted benzene. *Angew. Chem. Int. Ed.* **2000**, 39, 3273-3276.

[7] Qian, W.; Rubin, Y. A parallel library of all seven A_2+ B_2 + C_2 T_h regioisomeric hexakisadducts of fullerene C60: inspiration from Werner's octahedral stereoisomerism. *Angew. Chem. Int. Ed.* **2000**, *39*, 3133-3137.

[8] Lee, K.; Lee, Ch. H.; Song, H.; Park, J. T.; Chang, H. Y.; Choi, M.-G. Interconversion between $\mu - \eta^2, \eta^2 - C_{60}$ and μ_3 - $\eta^2, \eta^2, \eta^2 - C_{60}$ on a carbido pentaosmium cluster framework. *Angew. Chem. Int. Ed.* **2000**, *39*, 1801-1804.

[9] Fässler, T.F.; Hoffmann, R.; Hoffmann, S.; Wörle, M. Triple-Decker type coordination of fullerene trianion in [K([18] crown-6)]$_3$-[η^6, η^6 – C_{60}](η^3- $C_6H_5CH_3$)$_2$ – single crystal structure and magnetic properties *Angew. Chem. Int. Ed.* **2000**, *39*, 2091-2094.

[10] Kirby, E. C. Cylindrical and toroidal polyhex structures. *Croat. Chem. Acta*, **1993**, *66*, 13-26.

[11] Kirby, E. C.; Mallion, R. B.; Pollak, P. Toroidal polyhexes. *J. Chem. Soc. Faraday Trans.* **1993**, *89*, 1945-1953.

[12] Randić, M.; Tsukano, Y.; Hosoya, H. Kekule structures for benzenoid tori. *Natural Science Report, Ochanomizu University*, **1994**, *45*, 101-119.

[13] Kirby, E. C. On toroidal azulenoids and other shapes of fullerene cage. *Fullerene Sci. Technol.* **1994**, *2*, 395-404.

[14] Yoshida, M.; Fujita, M.; Fowler, P. W.; Kirby, E. C. Non-bonding orbitals in graphite, carbon tubules, toroids and fullerenes. *J. Chem. Soc. Faraday Trans.* **1997**, *93*, 1037-1043.

[15] Kirby, E. C.; Pollak, P. How to enumerate the connectional isomers of a toroidal polyhex fullerene. *J. Chem. Inf. Comput. Sci.* **1998**, *38*, 66-70.

[16] John, P. E. Kekule count in toroidal hexagonal carbon cages. *Croat. Chem. Acta,* **1998**, *71*, 435-447.

[17] Graovac, A.; Kaufman, M.; Pisanski, T.; Kirby, E. C.; Plavšić, D. On nodal properties of torusenes. *J. Chem. Phys.* **2000**, *113*, 1-7.

[18] Ceulemans, A.; Chibotaru, L. F.; Bovin, S. A.; Fowler, P. W. The electronic structure of polyhex carbon tori. *J. Chem. Phys.* **2000**, *112*, 4271-4278.

[19] Marušić, D.; Pisanski, T. Symmetries of hexagonal molecular graphs on the torus. *Croat.Chem. Acta*, **2000**, *73*, 969-981.

[20] Kirby, E. C. On the partially random generation of fullerenes. *Croat.Chem. Acta*, **2000**, *73*, 983-991.

[21] Iijima, S, Helical microtubules of graphitic carbon. *Nature* (London), **1991**, *354*, 56-58.

[22] Liu, J.; Dai, H.; Hafner, J. H.; Colbert, D. T.; Smalley, R. E.; Tans, S. J.; Dekker, C. Fullerene "crop circles". *Nature*, **1997**, *385*, 780-781

[23] Graovac, A.; Plavšić, D.; Kaufman, M.; Pisanski, T.; Kirby, E. C. Application of the adjacency matrix eigenvectors method to geometry determination of toroidal carbon molecules. *J. Chem. Phys.* **2000**, *113*, 1925-1931.

[24] Manolopoulos, D. E.; Fowler, P. W. Molecular graphs, point groups, and fullerenes. *J. Chem. Phys.* **1992**, *96*, 7603-7614.

[25] Fowler, P. W.; Pisanski, T.; Shawe-Taylor, J., in *Graph Drawing*, Tamassia, R.; Tollis, I. G., Eds., Lecture Notes in Computer Science, Springer, Berlin, 1995, pp. 282, 894.

[26] Diudea, M. V.; Graovac, A.; Kerber, A. Generation and graph-theoretical properties of C_4-tori. *Commun. Math. Comput. Chem.* (*MATCH*), this volume.

[27] Pisanski, T.; Žitnik, A.; Graovac, A.; Baumgartner, A. Rotagraphs and their generalizations, *J. Chem. Inf. Comput. Sci.* **1994**, *34*, 1090-1093.

[28] Gao, Y. D.; Herndon, W. C. Fullerenes with four-membered rings. *J. Amer. Chem. Soc.* **1993**, *115*, 8459-8460.

[29] Liu, X.; Klein, D. J.; Schmaltz, T. G. Preferable fullerenes and Clar-sextet cages. *Fullerene Sci. Technol.* **1994**, *2*, 405-422.

[30] King, R. B. Applications of Graph Theory and Topology in Inorganic Cluster and Coordination Chemistry, CRC Press, 1993.

[31] Diudea, M. V.; John, P. Covering polyhedral tori. *Commun. Math. Comput. Chem.* (*MATCH*), this volume.

[32] Diudea, M.V.; Parv, B.; Graovac, A.; Pisanski, T. Square and Polyhex Tori: A Common Building. (manuscript in preparation).

[33] Liu, X.; Klein, D. J.; Schmaltz, T. G. Preferable fullerenes and Clar-sextet cages. *Fullerene Sci. Technol.* **1994**, 2, 405-422.

[34] Schmalz, T. G.; Seitz, W. A.; Klein, D. J.; Hite, G. E. Elemental carbon cages. *J. Am. Chem. Soc.* 1988, 110, 1113-1127.

[35] Fowler, P. W.; Heine, T.; Manolopoulos, D. E.; Mitchell, D.; Orlandini, G.; Schmidt, R.; Seiferth, G.; Zerbetto, F. Energetics of fullerenes with four-membered rings. *J. Phys. Chem.* **1996**, *100*, 6984-6991]

[36] Jensen, J. F.; Toflund, H., Structure and Stability of C_{24} and $B_{12}N_{12}$ isomers, *Chem. Phys. Lett.* **1993**, *201*, 84;

[37] Silaghi-Dumitrescu, I. Haiduc, I.; Sowerby, D. B. Fully inorganic (Carbon-free) fullerenes. The Boron-Nitrogen case. *Inorg. Chem.* **1993**, *32*, 3755-3758.

[38] Silaghi-Dumitrescu, I.; Lara-Ochoa, F.; Bishof, P.; Haiduc, I. More about boron-nitrogen $B_{12+3n}N_{12+3n}$ fullerene-like cages. An ab initio and AM1 investigation of some 4/6 series, *J. Mol. Struct.* (*Theochem*), **1996**, *367*, 47-54.

[39] Scuseria, G. E. Ab initio theoretical predictions of fullerenes. In Billups, W. E.; Ciufolini, M. A. (Eds.), Buckminsterfullerenes, VCH, Weinheim, **1993**, p.108;

[40] Stewart, J. J. P. Optimization of parameters for semiempirical methods. I. Method. *J. Comput. Chem.* **1989**, *10*, 209-220.

[41] Spartan, version 5.1, Wavefunction, Inc. Suite 370, Irvine, CA 92612, USA

[42] Schmidt, M. W., Boldrige, K. K., Boatz, I. A.; Elbert, S. T.; Koseki, S.; Matsunaga, N; Nguyen, K. A.; Su, S. I.; Windus, Dupuis, M.; Montgomery, I. A. *J. Comput. Chem.* **1993**, *14*, 1347-1363.

[43] HyperChem [TM], release 4.5 for SGI, © 1991-1995, HyperCube, Inc.